VOLUME 34 | SUPPLEMENT 2 | MARCH 2021

MODERN PATHOLOGY

ABSTRACTS

NEUROPATHOLOGY AND OPHTHALMIC PATHOLOGY

(848-862)

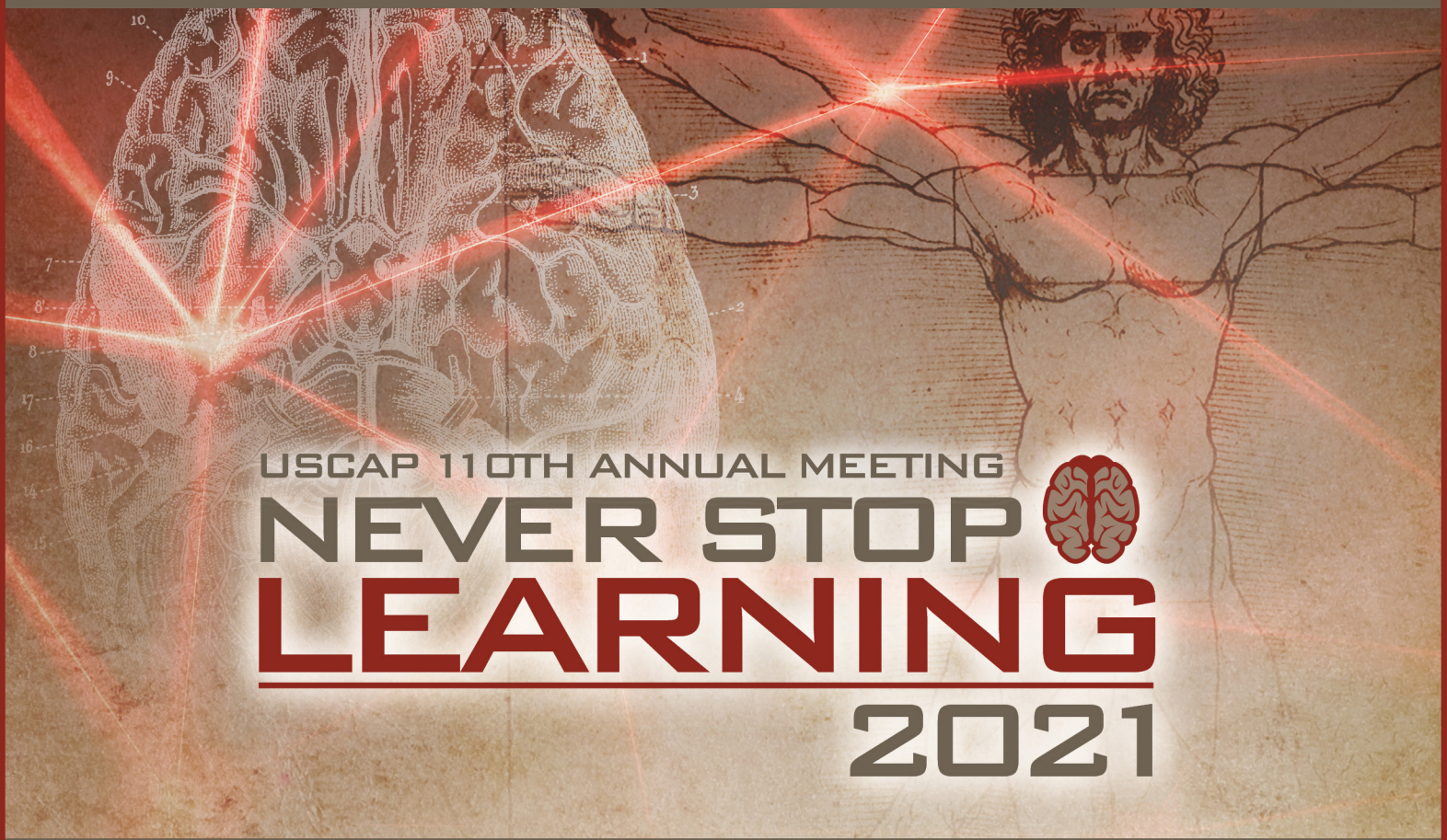

MARCH 13-18, 2021 | VIRTUAL AND INTERACTIVE

Published by
SPRINGER NATURE
www.ModernPathology.org

USCAP
Creating a Better Pathologist
AN OFFICIAL JOURNAL OF THE UNITED STATES AND CANADIAN ACADEMY OF PATHOLOGY

EDUCATION COMMITTEE

Jason L. Hornick
Chair

Rhonda K. Yantiss, Chair
Abstract Review Board and Assignment Committee

Kristin C. Jensen
Chair, CME Subcommittee

Laura C. Collins
Interactive Microscopy Subcommittee

Raja R. Seethala
Short Course Coordinator

Ilan Weinreb
Subcommittee for Unique Live Course Offerings

David B. Kaminsky
(Ex-Officio)
Zubair W. Baloch
Daniel J. Brat
Sarah M. Dry
William C. Faquin
Yuri Fedoriw
Karen Fritchie
Jennifer B. Gordetsky
Melinda Lerwill
Anna Marie Mulligan
Liron Pantanowitz
David Papke,
Pathologist-in-Training
Carlos Parra-Herran
Rajiv M. Patel
Deepa T. Patil
Charles Matthew Quick
Lynette M. Sholl
Olga K. Weinberg
Maria Westerhoff
Nicholas A. Zoumberos,
Pathologist-in-Training

ABSTRACT REVIEW BOARD

Benjamin Adam
Rouba Ali-Fehmi
Daniela Allende
Ghassan Allo
Isabel Alvarado-Cabrero
Catalina Amador
Tatjana Antic
Roberto Barrios
Rohit Bhargava
Luiz Blanco
Jennifer Boland
Alain Borczuk
Elena Brachtel
Marilyn Bui
Eric Burks
Shelley Caltharp
Wenqing (Wendy) Cao
Barbara Centeno
Joanna Chan
Jennifer Chapman
Yunn-Yi Chen
Hui Chen
Wei Chen
Sarah Chiang
Nicole Cipriani
Beth Clark
Alejandro Contreras
Claudiu Cotta
Jennifer Cotter
Sonika Dahiya
Farbod Darvishian
Jessica Davis
Heather Dawson
Elizabeth Demicco
Katie Dennis
Anand Dighe
Suzanne Dintzis
Michelle Downes
Charles Eberhart
Andrew Evans
Julie Fanburg-Smith
Michael Feely
Dennis Firchau
Gregory Fishbein
Andrew Folpe
Larissa Furtado
Billie Fyfe-Kirschner
Giovanna Giannico
Christopher Giffith
Anthony Gill
Paula Ginter
Tamar Giorgadze
Purva Gopal
Abha Goyal
Rondell Graham
Alejandro Gru
Nilesh Gupta
Mamta Gupta
Gillian Hale
Suntrea Hammer
Malini Harigopal
Douglas Hartman
Kammi Henriksen
John Higgins
Mai Hoang
Aaron Huber
Doina Ivan
Wei Jiang
Vickie Jo
Dan Jones
Kirk Jones
Neerja Kambham
Dipti Karamchandani
Nora Katabi
Darcy Kerr
Francesca Khani
Joseph Khoury
Rebecca King
Veronica Klepeis
Christian Kunder
Steven Lagana
Keith Lai
Michael Lee
Cheng-Han Lee
Madelyn Lew
Faqian Li
Ying Li
Haiyan Liu
Xiuli Liu
Lesley Lomo
Tamara Lotan
Sebastian Lucas
Anthony Magliocco
Kruti Maniar
Brock Martin
Emily Mason
David McClintock
Anne Mills
Richard Mitchell
Neda Moatamed
Sara Monaco
Atis Muehlenbachs
Bita Naini
Dianna Ng
Tony Ng
Michiya Nishino
Scott Owens
Jacqueline Parai
Avani Pendse
Peter Pytel
Stephen Raab
Stanley Radio
Emad Rakha
Robyn Reed
Michelle Reid
Natasha Rekhtman
Jordan Reynolds
Andres Roma
Lisa Rooper
Avi Rosenberg
Esther (Diana) Rossi
Souzan Sanati
Gabriel Sica
Alexa Siddon
Deepika Sirohi
Kalliopi Siziopikou
Maxwell Smith
Adrian Suarez
Sara Szabo
Julie Teruya-Feldstein
Khin Thway
Rashmi Tondon
Jose Torrealba
Gary Tozbikian
Andrew Turk
Evi Vakiani
Christopher VandenBussche
Paul VanderLaan
Hannah Wen
Sara Wobker
Kristy Wolniak
Shaofeng Yan
Huihui Ye
Yunshin Yeh
Anjana Yeldandi
Gloria Young
Lei Zhao
Minghao Zhong
Yaolin Zhou
Hongfa Zhu

To cite abstracts in this publication, please use the following format: **Author A, Author B, Author C, et al. Abstract title (abs#). In "File Title."** ***Modern Pathology*** **2021; 34 (suppl 2): page#**

848 Comparison of PRAME Immunohistochemistry (IHC) and PRAME RT-PCR in 14 Uveal Melanomas

Saman Ahmadian[1], Angus Toland[1], Romain Cayrol[2], Peter Egbert[1], Donald Born[3], Ryanne Brown[4], Jonathan Lin[1], Prithvi Mruthyunjaya[1]
[1]Stanford Health Care, Stanford, CA, [2]Montreal, Canada, [3]Stanford University, Stanford, CA, [4]Stanford Medicine/Stanford University, Stanford, CA

Disclosures: Saman Ahmadian: None; Peter Egbert: None; Donald Born: None; Ryanne Brown: None; Jonathan Lin: None

Background: Uveal melanomas are the most common primary intraocular malignancy in the adult population. Based on the gene expression profiles, uveal melanomas can be prognostically categorized as Class 1 (low risk for metastasis) or Class 2 (high risk for metastasis). PRAME (PReferentially expressed Antigen in MElanoma) protein is a member of the cancer-testis antigen family. PRAME is not expressed at appreciable levels in normal melanocytes but can be markedly induced on the nucleus of malignant melanocytes in cutaneous and uveal melanomas. PRAME is an independent prognostic biomarker in uveal melanomas. Clinical trials are ongoing to test the efficacy of anti-PRAME immunotherapy in melanomas. RT-PCR is commonly used to detect PRAME in uveal melanoma samples. More recently, PRAME protein immunohistochemistry (IHC) has also been validated for uveal melanomas. However, it is unclear which testing modality, PCR or IHC, should be used for assessing PRAME expression in uveal melanomas. Here, we compared PRAME expression using RT-PCR and IHC in 14 uveal melanoma cases.

Design: Among 17 patients with RT-PCR results for PRAME expression performed at Castle BioScience Inc. (Friendswood, Texas, USA), we were able to retrieve FFPE blocks for 14 cases. Immunohistochemistry against anti-PRAME monoclonal antibody (mAb) (EPR20330 Abcam, #219650) was performed on these cases and the results compared to the RT-PCR results.

Results: The cohort included 14 patients (11 men; 3 women) with an average age = 60.2 (range from 37 to 80). Eleven out of 14 cases showed concordant PRAME results by RT-PCR and IHC. Interestingly, three out of 14 cases showed discordant results with negative results for PRAME by IHC and positive results by RT-PCR. From these three cases, two cases were categorized as low risk for metastasis (class 1b), and one case was high risk for metastasis (class 2). None of these 3 cases showed metastasis in the follow-up duration (3, 7, and 17 months).

Conclusions: Our findings reveal that PRAME RT-PCR and PRAME IHC provide concordant results in the majority of cases (11/14 in our cohort). However, discordant results between PRAME RT-PCR and PRAME IHC were observed in a small fraction (3/14). We propose that the discordant results for PRAME RT-PCR testing and PRAME IHC may be due to a lack of PRAME expression at the protein level but not in mRNA expression. Further study is necessary to determine the prognostic implications of discordant PRAME results by IHC and RT-PCR in uveal melanoma.

849 Comprehensive Molecular Testing Identified Targetable Novel and Rare Genomic Alterations in Brain Tumors

Rofieda Alwaqfi[1], Deqin Ma[1]
[1]University of Iowa Hospitals & Clinics, Iowa City, IA

Disclosures: Rofieda Alwaqfi: None; Deqin Ma: None

Background: The most recent WHO classification of central nerve system (CNS) tumors incorporated genomic aberrations into tumor classification. Molecular findings also have prognostic and therapeutic implications. Mutation analysis for *IDH* and *BRAF*, FISH study for 1p/19q loss, and MGMT promoter methylations are routinely performed in many institutions for brain tumors. In comparison, other than BRAF fusions, the correlation of gene fusions with brain tumors is less well established. We studied 123 brain tumors and identified rare and novel gene fusions which are potentially targetable and correlated the molecular findings with pathologic diagnosis.

Design: Brain tumors from 123 patients were tested. Total RNA was extracted from formalin-fixed, paraffin-embedded tissue (Qiagen RNeasy FFPE mini kit). 200ng RNA was used for targeted library preparation.

Targeted sequencing for gene fusions were performed using the Archer FusionPlex Lung Thyroid Panel (ArcherDX) on an Illumina MiSeq.

Results: Eight different fusions were identified in 87 tumors. Seventy-nine cases had *KIAA1549-BRAF* fusion. Rare and novel fusions included a *TRAK1-RAF1* fusion in a desmoplastic infantile ganglioglioma from a 10-month-old female with Prader-Willi syndrome, a *BCR-NTRK2* fusion in a 52 year-old-male with a low-grade infiltrating astrocytoma, a *BCAN-NTRK1* fusion in a 18-year old with glioblastoma, and a *INA-FGFR2* fusion in a 15-year-old male who has a histopathologic diagnosis of low grade mixed neuronal-glial tumor. Two *BRAF* gene rearrangements with different fusion partners (*PRKAR2B-BRAF*, a novel fusion, and *TOP2B-BRAF*) were identified in two cases of low grade glioneuronal tumors. In addition, a *PTPRZ1-MET* fusion which has only been reported in grade III astrocytoma and secondary glioblastoma was identified in a 59-year-old patient with Grade 4 primary glioblastoma. Of note, all these fusions have FDA approved drug such as NTRK, BRAF, FGFR inhibitors or RET, RAF, and MET inhibitors that might be used for treatment. Table 1.

Table 1. Rare and Novel Fusions Identified in Brain Tumors

Histopathologic Diagnosis	Age(year)/ Gender	Fusion Detected	Number of Cases	Therapy
Desmoplastic infantile ganglioglioma	< 1M	*TRAK1/RAF1*	1	RAF inhibitor
Low grade infiltrating astrocytoma	52 M	*BCR/NTRK2*	1	NTRK inhibitor
Glioblastoma Grade 4	18 M	*BCAN/NTRK1*	1	NTRK inhibitor
Low grade mixed neuronal-glial tumor	15 M	*INA/FGFR2*	1	FGFR2 inhibitor
Low grade glioneuronal tumor	23 F	*PRKAR2B/BRAF*	1	BRAF inhibitor
Low grade glioneuronal tumor	16 M	*TOPO2B/BRAF*	1	BRAF inhibitor
Glioblastoma, IDH-wild-type	39	*PTPRZ1/MET*	1	RET inhibitor

Conclusions: Our results demonstrated the importance of thorough molecular examination of all newly diagnosed brain tumors. Similar to mutations, gene fusions can serve as oncogenic drivers in brain tumors as well as therapeutic targets. Patients with tumors that harbor specific gene fusions may be treated with emerging targeted therapies.

850 Hypoxia-Inducible Factor-1α in Tumorigenesis of Lacrimal Gland Adenoid Cystic Carcinoma

Shahzan Anjum[1], Seema Sen[1], Kunzang Chosdol[1], Sameer Bakhshi[1], Seema Kashyap[1], Neelam Pushker[1]
[1]All India Institute of Medical Sciences, New Delhi, India

Disclosures: Shahzan Anjum: None; Seema Sen: None; Kunzang Chosdol: None; Sameer Bakhshi: None; Seema Kashyap: None; Neelam Pushker: None

Background: Lacrimal gland adenoid cystic carcinoma (ACC) is a rare, aggressive tumor with high risk of recurrence and distant metastasis. Hypoxia is the most common feature in solid tumor progression and therefore has become a central issue in cancer treatment. Hypoxia- inducible factor-1α (HIF-1α) makes the tumor produce adaptive biological response to hypoxia and become more aggressive. The present study was designed to evaluate the status of HIF-1α in lacrimal gland ACC and to correlate with clinicopathological features.

Design: Twenty- eight patients of histopathologically proven lacrimal gland ACC and five normal lacrimal gland tissues were included in this study. Fresh tissues were available in 14 cases. TNM staging was done according to AJCC guidelines(8th edition). Follow-up was available in all patients. Immunoexpression of HIF-1α was evaluated by immunohistochemistry (IHC) using monoclonal antibody (mgc3, Invitrogen) in all 28 cases. mRNA expression analysis of HIF-1α gene was done in 14 cases by real time PCR using SYBR green chemistry. The results obtained were correlated with clinicopathological features and survival of the patients. Kaplan-Meier survival and multivariate analysis was performed to determine the prognostic significance.

Results: Of the 28 ACC cases there were 14 females and 14 males with a mean age of 34.8 years (±17.5). Orbital imaging showed presence of intracranial extension in 5(18%) and bone erosion in 10(36%) cases. Histologically, large tumor >25mm was observed in 21(75%), solid histologic pattern in 10(36%), cribriform in 15(54%), tubular in 3(11%) and perineural invasion in 10(36%) cases. Nuclear positivity of HIF-1α protein was detected in 12 of 28 cases (43%), and HIF-1α mRNA in 3 of 14 cases (21.4%).There was no significant correlation between the immuno and mRNA expression of HIF-1α. HIF-1α immunoexpression was significantly associated with advanced tumor stage(T3-T4) and mRNA with perineural invasion. On Kaplan Meier survival analysis bone erosion, solid histologic pattern, perineural invasion, intracranial extension, exenteration and nuclear immunoexpression of HIF-1α significantly correlated with reduced disease free survival. However, there was no significant correlation with HIF-1α mRNA. Bone erosion, solid histologic pattern, perineural invasion, intracranial extension, and exenteration were indicators of poor prognosis. By multivariate analysis solid histologic pattern (HR: 8.4, 95% CI:1.9-37.5, P=0.005) and bone erosion (HR: 5.9, 95% CI: 1.3-26.9, P=0.02) were found to be the most significant poor prognostic indicators.

Conclusions: Overexpression of HIF-1α protein was significantly associated with reduced disease free survival. Solid histologic pattern and bone erosion were the most important predictors of poor outcome. HIF-1α as a potential novel therapeutic target in the management of aggressive lacrimal gland ACC needs to be explored.

851 Approach to a Reflex-Based Meningitis Testing Pathway

Ryan Beaver[1], Priscilla Powell[2], Matthew Brigmon[1], Patrick Crowley[1], Hannakate Lichota[3], Kimberly Walker[2], Lizbeth Cahuayme-Zuniga[1], Arundhati Rao[2], Manohar Mutnal[1]
[1]Baylor Scott & White Medical Center, Temple, TX, [2]Baylor Scott & White Health, Temple, TX, [3]Baylor Scott & White Health/Texas A & M Health Science Center College of Medicine, Temple, TX

Disclosures: Ryan Beaver: None; Priscilla Powell: None; Matthew Brigmon: None; Patrick Crowley: None; Hannakate Lichota: None; Kimberly Walker: None; Lizbeth Cahuayme-Zuniga: None; Arundhati Rao: None; Manohar Mutnal: None

Background: The documented overuse of the meningitis-encephalitis multiplex polymerase chain reaction (ME-PCR) panel has led to an abundance of negative tests, at considerable cost, but without a significant shift in subsequent clinical decision making. We aim to investigate whether a reflex-based approach can improve diagnostic stewardship without compromising patient safety.

Design: Baseline inclusion criteria required CSF samples to have a WBC differential and concurrent collection of CSF culture and ME-PCR panel. Organisms not possibly detectable by the ME-PCR assay were excluded *a priori*, as were patients with large radiographic intracranial hemorrhage on admission. Retrospective chart review divided adult patients into true positive (TP) and true negative (TN) groups by requiring both laboratory diagnostic and clinical discharge diagnosis concordance of results; discordant pairs were excluded to reduce confounding. CSF biochemical characteristics were compared in both univariate and multivariate approaches, and cut points for maximum sensitivity were established by receiver operating characteristic (ROC) curves using SAS 9.4. Statistical analysis for sensitivity, specificity, positive predictive value (PPV), negative predictive value (NPV), and a theoretical utilization reduction potential was calculated for each reflex approach. High sensitivity and negative predictive value will serve as markers of patient safety.

Results: 1210 charts were retrospectively screened. 108 were excluded (97 for missing data, 11 for brain hemorrhage), and 199 for discordant laboratory and clinical results. The remaining 903 were divided into 72 TP and 831 TN. The three reflex strategies are compared in **Table 1**, with subgroup analysis for bacterial, viral, and fungal classification. A traditional reflex approach (defined as abnormal WBC > 5) had the highest universal sensitivity at 95.8% and NPV 99.6%. A univariate approach using a statistical WBC cut point had a sensitivity of 93.1% and NPV 99.3%, and a multivariate approach using continuous variables for WBC, glucose, protein, and lymphocyte percentage had a sensitivity of 83.3%, NPV 98.5%. Theoretical utilization reduction potential ranged from 74.9% to 86.1%.

Table 1. Comparison of Univariate and Multivariate Approaches to a Reflexive CSF/ME-PCR Diagnostic Pathway

	Sensitivity	Specificity	PPV	NPV	AUC	Utilization Reduction
All Organisms (n = 72)						
Univariate: Traditional	95.8%	81.0%	30.4%	99.6%	0.884	74.9%
Univariate: Cutpoint (WBC > 8)	93.1%	88.7%	41.6%	99.3%	0.909	82.2%
Multivariate: Continuous	83.3%	92.1%	47.6%	98.5%	0.877	86.1%
Bacterial (n = 15)						
Univariate: Traditional	93.3%	81.0%	8.1%	99.9%	0.872	79.7%
Univariate: Cutpoint (WBC > 15)	93.3%	93.7%	21.2%	99.9%	0.935	92.2%
Multivariate: Continuous	86.7%	91.5%	15.5%	99.7%	0.891	90.1%
Viral (n = 49)						
Univariate: Traditional	95.9%	81.0%	22.9%	99.7%	0.885	76.7%
Univariate: Cutpoint (WBC > 8)	93.9%	88.7%	32.9%	99.6%	0.913	84.1%
Multivariate: Continuous	81.6%	92.7%	39.6%	98.8%	0.872	88.5%
Fungal (n = 8)						
Univariate: Traditional	100.0%	81.0%	4.8%	100.0%	0.905	80.2%
Univariate: Cutpoint (WBC > 7)	100.0%	87.4%	7.1%	100.0%	0.937	86.5%
Multivariate: Continuous	75.0%	99.4%	54.6%	99.8%	0.872	98.7%

N = 903 samples. True Positive = 72. True Negative = 831.
Univariate Traditional: Reflex if WBC > 5.
Univariate Cutpoint: Reflex if WBC > calculated ROC curve max sensitivity cutpoint for variable of WBC only.
Multivariate Continuous: Reflex if > ROC curve cutpoint using variables of WBC, protien, glucose, and %lymphocytes
Utilization Reduction: Percentage of tests not performed for a given reflex strategy.

Conclusions: A reflex-based approach is both a possible and practical answer to improving the diagnostic stewardship of the ME-PCR panel, significantly decreasing unnecessary cost and utilization without impacting patient safety compared to stand-alone ordering practice.

852 Orbital Exenterations: Standardization of the Gross Examination

Elizabeth Cheek[1], Ruifeng (Ray) Guo[1], Diva Salomao[1]
[1]Mayo Clinic, Rochester, MN

Disclosures: Elizabeth Cheek: None; Ruifeng (Ray) Guo: None; Diva Salomao: None

Background: Orbital exenterations (OEs) are uncommon and challenging surgical pathology specimens. Few pathology resources exist to provide guidance on the proper handling of the spectrum of malignancies arising in the complex anatomical structures. Utilizing a systematic review of OEs at our institution, we describe our experience with grossing these specimens and impact on management.

Design: A total of 76 cases of OEs were identified from archived material from 2005-2020, with the primary tumors from skin (33), conjunctiva (12), sinonasal (13), nasaolacrimal duct (4), and others (14). The focus was on evaluating gross features, margin status and post-operative management. 35/76 cases had complete patient follow-up. The impact was measured with quality metrics in final pathology reports and clinical management.

Results: Despite the complexity of these specimens, 0/76 cases required additional tissue submission or report modification due to insufficient gross examination. We reviewed margin status, location of positivity and subsequent adjuvant treatment. Our standardized protocol facilitated adequate and accurate sampling of tumor margins in all cases, ensuring no critical margins were missed. In 51/76 cases, when gross lesions were identified, they were accurately described and incorporated into the diagnosis. Specific structures involved by tumors were appropriately documented and evaluated, impacting staging and subsequent management. Standard block diagram creation in 2020 also aided in ease of section and positive margin location (Please see Images 1 and 2). Only 2/26 patients with reported negative margins had recurrences. In contrast, 5/10 patients with positive margins had disease recurrences, despite additional adjuvant therapy.

Figure 1 - 852

Figure 2 - 852

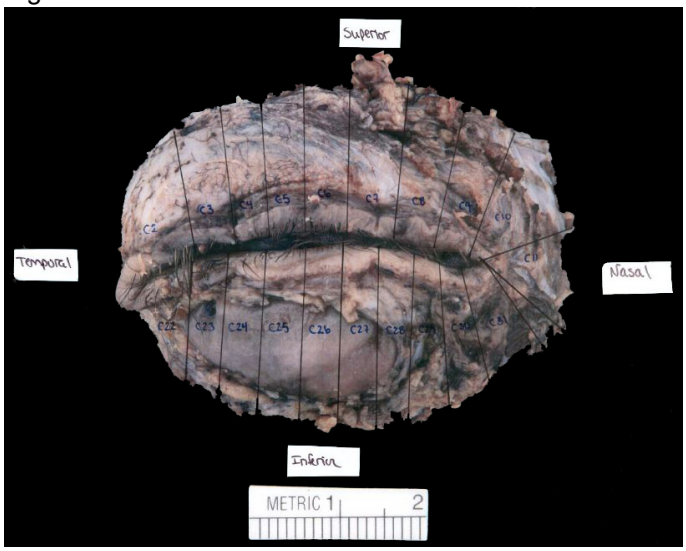

Conclusions: By our approach to macroscopic examination of these complex specimens, we demonstrate the importance of an adequate and standardized manner for appropriate orientation, processing, and sampling of OEs, which is critical in final pathology report and subsequent clinical utility.

853 Single Institutional Experience on Orbital Inflammatory Pseudotumor – Diagnostic and Management Challenge

Roshanak Derakhshandeh[1], Yiannis Petros Dimopoulos[1], Haideh Sabet[1], Metin Ozdemirli[2]
[1]MedStar Georgetown University Hospital, Washington, DC, [2]Georgetown University, Washington, DC

Disclosures: Roshanak Derakhshandeh: None; Yiannis Petros Dimopoulos: None; Haideh Sabet: None; Metin Ozdemirli: None

Background: Orbital inflammatory pseudotumor (OIP) also known as idiopathic orbital inflammatory syndrome, is considered a reactive and non-neoplastic inflammatory process. Infectious and immune-mediate etiologies have been proposed. Clinically, it may present a localized or a diffuse process, involving orbital structures and fat and masquerading as a mass/malignancy. Since clinical and radiological manifestations could mimic a neoplastic process a histological evaluation is crucial. Histologically, it is associated with chronic inflammation, plasmacytosis and variable degrees of sclerosis. We sought to investigate potential B and T-cell clonality in cases pathologically diagnosed as OIP.

Design: The cases diagnosed as OIP in our department in the past 15 years have been re-examined. Hematoxylin and eosin stained slides, immunohistochemically stained slides (for CD138, IgG, IgG4, CD20, CD3), and polymerase chain reactions (PCR) on cell block material for the investigation of clonality of B (Ig-Heavy and Ig-kappa) and T (TCR-beta and TCR-gamma) cell receptors were reviewed (or performed in cases they were missing) to confirm the diagnosis and investigate the prevalence of concomitant diseases. Clinical charts were additionally reviewed for basic demographic data and clinical follow up.

Results: A total of 13 cases of OIP were identified, with one case representing a recurrence. The majority of patients were female (70%). Age ranged from 23 to 79, with an average age of 51 years. Histologically, the lesions exhibited a various degree of lymphoplasmacytic infiltrate with a sclerotic background. Immunohistochemical analysis with CD138, IgG, and IgG4 showed varying numbers of plasma cells in each case. Five cases (5/13, 38%) exhibited relative increase in the presence of IgG4 plasma cells, with 2 cases reaching diagnostic criteria for IgG4-related disease (IgG4rD) (2/13, 15%). PCR analysis on cell blocks showed clonal B cell populations in 2 cases (2/13, 15%). Additionally, PCR analysis in the patient with disease recurrence failed to reveal clonality. There were no clinical reports of recurrence or progression to lymphoma in any of the patients (average follow up of 223 days).

Table 1. Basic demographic data of the patients as well as the prevalence of IgG4rD and B and T cell clonality.

Characteristics	n (%)
Total patients	13
Male	4 (30)
Female	9 (70)
Age (Year)	
Mean	51
Median	55
Range	23-79
IgG4	
Increased IgG4	5 (38)
IgG4/IgG >40%	2 (15)
Clonality	
B-cell (IgH, Igk)	2 (15)
T-cell (TCRb, TCRg)	0 (0)

Conclusions: A small but significant percentage of typical OIP on pathology showed B cell clonality on PCR analysis of B-cell receptors and development of IgG4rD. Close follow up of these patients to identify potential lymphoma or systemic IgG4rD respectively may be clinically warranted.

854 Genomic Landscape of Primary CNS Large B-cell Lymphoma in Children and Young Adults is Distinct from Older Adults

Ekin Guney[1], Calixto-Hope Lucas[1], Ruth Zhang[1], Robert Ohgami[1], Roberto Ruiz-Cordero[1], James Rubenstein[1], Daniel Boue'[2], Kristian Schafernak[3], Gerald Wertheim[4], Andrew Bollen[1], Arie Perry[1], Tarik Tihan[1], Melike Pekmezci[1], David Solomon[1], Kwun Wah Wen[1]
[1]University of California, San Francisco, San Francisco, CA, [2]Nationwide Children's Hospital - The Ohio State University, Columbus, OH, [3]Phoenix Children's Hospital, Phoenix, AZ, [4]Children's Hospital of Philadelphia, University of Pennsylvania, Philadelphia, PA

Disclosures: Ekin Guney: None; Calixto-Hope Lucas: None; Ruth Zhang: None; Robert Ohgami: None; Roberto Ruiz-Cordero: None; James Rubenstein: None; Daniel Boue': None; Kristian Schafernak: None; Gerald Wertheim: None; Andrew Bollen: None; Arie Perry: None; Tarik Tihan: None; Melike Pekmezci: None; David Solomon: None; Kwun Wah Wen: None

Background: Primary central nervous system large B-cell lymphoma (CNS-LBCL) typically occurs in older adults and only rarely in the pediatric population. Pediatric patients appear to have a better overall prognosis, suggesting the possibility that CNS-LBCL may be biologically and genetically divergent between children and adults. However, the genomic landscape and molecular underpinnings of CNS-LBCL in children, adolescents, and young adults (AYA) are not well-characterized.

Design: We reviewed clinical and pathologic data and performed capture-based next generation sequencing (NGS) of ~500 cancer-associated genes on pathologically-confirmed CNS-LBCL from 17 pediatric and AYA patients in this multi-institutional study.

Results: The median age and mean age at diagnosis of the 17 patients (10 females, 7 males) were 25 years and 24 years (range 7-40 years). Genomic analysis segregated these tumors into three molecular groups: Group 1 ("pediatric-type") (n=8, mean age 13 years, range 7-17 years) was characterized by frequent alterations in *TP53* (5/8, 63%), *NFKBIE* (3/8, 38%), *GNA13* (4/8, 50%), and *GATA2* (2/8, 25%), with an absence of *MYD88* mutations. Group 2 ("adult-type, *MYD88*-mutant") (n=4, mean age 33 years, range 25-38 years) was defined by *MYD88* mutations (4/4, 100%), with frequent mutations or deletions of *PRDM1* (3/4, 75%) and homozygous deletion of *CDKN2A/B* (3/4, 75%). Group 3 ("adult-type, *MYD88*-wildtype") (n=5, mean age 35 years,

range 25-40 years) lacked *MYD88* mutations and enrichment for those genetic alterations seen in Group 1 tumors. Kaplan-Meyer analysis demonstrated better overall survival for children and AYA with pediatric type Group 1 tumors compared to their older counterparts, but this did not reach statistical significance due to the small cohort size.

Conclusions: We identified a "pediatric-type" molecular subgroup of CNS-LBCL that is genetically distinct from its adult counterpart based on an absence of *MYD88* mutations as well as an enrichment for *TP53*, *NFKBIE*, and *GNA13* mutations and *GATA2* homozygous deletion. A subset of AYA patients had tumors with *MYD88* and *PRDM1* mutations characteristic of CNS-LBCL occurring in older adults, while another subset of AYA patients lacked this genetic signature and may potentially represent a third distinct subtype of CNS-LBCL. Our results lay the foundation for a genetic subclassification system for CNS-LBCL in children and AYA, and points toward a need for the development of specific treatment protocols in this unique patient population.

855 The Role of Alpha-B-Crystallin and p16 Accumulation in the Diagnosis and Pathogenesis of Focal Cortical Dysplasias

Ekin Guney[1], Tara Saunders[1], Calixto-Hope Lucas[1], Daniel Sullivan[1], Melike Pekmezci[1], David Solomon[1], Andrew Bollen[1], Arie Perry[1], Tarik Tihan[1]
[1]University of California, San Francisco, San Francisco, CA

Disclosures: Ekin Guney: None; Tara Saunders: None; Calixto-Hope Lucas: None; Daniel Sullivan: None; Melike Pekmezci: None; David Solomon: None; Andrew Bollen: None; Arie Perry: None; Tarik Tihan: None

Background: Epilepsy is a common disorder with various etiologies showing overlapping morphologic features. Balloon cells (BCs) are a distinct feature of focal cortical dysplasia (FCD) International League against Epilepsy (ILAE) type IIB, and are thought to be in cellular senescence triggered by factors such as oxidative stress. Alpha-B-crystallin (ABC), a heat shock protein, and p16, a senescence marker, are reportedly upregulated in BCs in FCD IIB. However, the utility of these stains in epilepsy pathology is unknown.

Design: We retrospectively reviewed specimens from patients with FCDI (n=11), FCDIIA (n=13), FCDIIB (n=19), mesial temporal sclerosis (MTS) (n=10), astrogliosis (n=9), ganglioglioma (GG) (n=10), dysembryoplastic neuroepithelial tumor (DNET) (n=9), subependymal giant cell astrocytoma (SEGA) (n=7) and oligodendroglioma (OL) (n=10). We performed immunohistochemistry (IHC) for ABC and p16 on these specimens.

Results: The ABC stain showed strong cytoplasmic staining in dysmorphic neurons and BCs in FCDIIB (95%), but not in other non-neoplastic cases. There was variable glial cell staining in FCDIIB (11%), FCDIIA (23%), FCDI (91%), MTS (50%) and astrogliosis (11%). Staining for p16 showed a similar pattern but with more non-specific staining patterns in non-neoplastic epileptic disorder cases. In neoplastic cases, the ABC stain was positive in 86% of SEGA, showed diffuse weak to moderate staining in OL (100%) and moderate staining in small subsets of tumor cells in GG (55%) and DNET (78%). The p16 stain showed diffuse strong staining in tumor cells, astrocytes, oligodendrocytes and in the background at the tumor focus in neoplastic epileptic cases.

Conclusions: ABC IHC is highly sensitive and specific in distinguishing FCD2B from other non-neoplastic epileptic disorders but not from neoplastic diseases. IHC for p16 has similar sensitivity but less specificity in non-neoplastic epileptic disorders.

856 Role of CD97 in Glioblastoma Multiforme

Afreen Karimkhan[1], Nainita Bhowmick[1], Niklas Boess[1], Prabhjot Sekhon[1], Takamitsu Hattori[1], Alexis Corrado[1], Akiko Koide[1], Shohei Koide[1], Dimitris Placantonakis[1], Christopher Park[2]
[1]NYU Grossman School of Medicine, New York, NY, [2]NYU School of Medicine, New York, NY

Disclosures: Afreen Karimkhan: None; Prabhjot Sekhon: None; Takamitsu Hattori: None; Christopher Park: None

Background: Glioblastoma (GBM) is the most common and deadly primary brain malignancy in adults. Tumor propagation, brain invasion, and resistance to therapy critically depend on GBM stem-like cells (GSCs). Given the

aggressiveness and poor prognosis of GBM, it is imperative to find biomarkers that could also translate into novel drug targets. Along these lines, we have identified a cell surface antigen, CD97 (ADGRE5), an adhesion G protein-coupled receptor (GPCR), that is expressed on GBM cells but is absent from non-neoplastic brain tissue.

Design: We assessed CD97 mRNA and protein expression in patient-derived GBM samples and cultures using publicly available RNA-sequencing datasets and flow cytometry, respectively. To assess CD97 function, we utilized shRNA lentiviral constructs that target CD97 or scrambled shRNA (scr) with no predicted targets in the genome. We evaluated CD97 shRNA lentivirally transduced GBM cells for proliferation, apoptosis, and their ability to self-renew using clonogenic tumorsphere formation assays. Further, we utilized synthetic Abs (sAbs) generated against the extacellular domain (ECD) of CD97 to test for potential antitumor effects using patient-derived GBM cell lines.

Results: CD97 mRNA was expressed at high levels in all GBM's in the TCGA cohort. We found high levels of surface CD97 protein expression in 6/6 patient-derived GBM cell cultures, but not human neural stem cells. CD97 KD(knockdown) induced a significant reduction in cell growth in 3 independent GBM cell lines representing mesenchymal and proneural subtypes, which was accompanied by reduced (~20%) Ki67 staining and increased (~30%) apoptosis. Using three unique GBM patient-derived cultures, we found that CD97 KD attenuated the ability of GBM cells to initiate sphere formation by over 300 fold, consistent with an impairment in GSC self-renewal. Incubation of GBM cells with sAbs (20 mg/ ml) against the ECD of CD97 for 3 days induced GSC differentiation, as determined by the expression of GFAP and tubulin.

Conclusions: Loss of CD97 expression in patient-derived GBM cells markedly decreased proliferation, induced cell death, and reduced tumorsphere formation. sAbs against the ECD of CD97 induced differentiation, suggesting that sAbs that inhibit CD97 function will exhibit anti-tumor activity. Collectively, these findings indicate that CD97 is necessary to support the maintenance of human GBM cells and identify CD97 as a promising therapeutically targetable vulnerability in GBM.

857 Clinical, Pathologic, and Molecular Features of BAP-1 Mutated Uveal Melanoma

Austin McHenry[1], Minghao Zhong[2], John Sinard[2]
[1]Yale University, New Haven, CT, [2]Yale School of Medicine, New Haven, CT

Disclosures: Austin McHenry: None; Minghao Zhong: None; John Sinard: None

Background: Uveal melanoma (UM) is an unusual, highly aggressive malignancy with poor prognosis. Compared to cutaneous melanoma (CM), UM metastasis has been shown to occur within a relatively short time from diagnosis. UM-related mortality is between 26 and 37% by 5 years. Recently, mutations in the tumor suppressor gene BAP-1 in UM have been associated with high risk for metastasis.

Design: We evaluated 11 BAP-1 mutated melanomas (8 of uveal and 3 of cutaneous origin) for additional mutational profiling in concordance with clinical and histopathologic features. Formalin-fixed, paraffin embedded tissue sections were used for tumor dissection. Extracted DNA was sequenced using customized targeted 166 gene panel on the Ion Torrent platform (Thermo Fisher Scientific Inc.). Bioinformatics analyses were performed using Torrent Suite.

Results: The median age of the UM and CM patients was 60 (range 36-88) and 66 years (range 55-66), respectively. The F:M ratio was 1.6:1 and 2:1 for UM and CM, respectively. All UM patients had metastatic disease with an average disease specific survival of 85 months from diagnosis. One of the 8 BAP-1 mutated UM cases was germline-altered (c.542_543delTT; p.Phe181Ter); no additional targeted mutations were identified in this patient's melanoma. Of the remaining 7 UM patients, all demonstrated an additional mutually exclusive activating mutation in either GNA11 (n = 5) or GNAQ (n = 2); two patients harbored one additional mutation (either SFB1, or MYC-amplification); and one patient harbored three additional mutations (PTEN, NTRK2, and MYC-amplification). In contrast, CM tumors developed on average 5-6 additional mutations, including CDKN2A, TERT, TP53, NF1, RET, FBXW7, MYCN, NOTCH2, ARID1A, BRCA2, AXL, and MYC-amplification.

Conclusions: The prevalence of BAP1 mutation in UM is much higher than that in CM. Comprehensive mutational analysis of BAP-1 mutated UM reveals a distinct mutational profile from CM, showing little similarity in the overlap and number of additional genomic alterations. HDAC inhibitors, PARP inhibitors are potential targeted therapy

option in patients with somatic or germline *BAP1* mutations. Identification of BAP1 mutation in UM and CM is clinically important.

858 Detection of Rare and Novel Gene Fusions in Patients with Diffuse Glioma

Kentaro Ohara[1], Samantha McNulty[2], Hussein Alnajar[3], Andrea Sboner[1], Sun-Joong Kim[2], Feng He[1], Murat Yaylaoglu[2], Todd Druley[4], Jenny Xiang[1], Olivier Elemento, David Pisapia[1], Juan Miguel Mosquera[1]
[1]Weill Cornell Medicine, New York, NY, [2]ArcherDX, Inc., Boulder, CO, [3]NorthShore University HealthSystem, Evanston, IL, [4]Invitae Corporation, San Francisco, CA

Disclosures: Kentaro Ohara: None; Samantha McNulty: None; Hussein Alnajar: None; Andrea Sboner: None; Sun-Joong Kim: None; Feng He: None; Murat Yaylaoglu: None; Todd Druley: *Employee*, ArcherDX/Invitae Corporation; *Stock Ownership*, ArcherDX/Invitae Corporation; Jenny Xiang: None; Olivier Elemento: *Stock Ownership*, Volastra Therapeutics; *Stock Ownership*, OneThree Biotech; Juan Miguel Mosquera: None

Background: Diffuse glioma is a genetically heterogeneous disease, often including multiple classes of genetic variants. Gene fusions are increasingly recognized as important oncogenic events that define molecular subgroups and inform targeted strategies. RNA sequencing (RNA-seq) is an efficient approach to identify new rare fusion transcripts. Using this method, our group identified a novel *BCOR-CREBBP* fusion in pediatric infiltrating astrocytoma (*Acta Neuropathol Commun* 2020). Here we present further experience in detecting novel gene fusions using both un-targeted (RNA-seq) and targeted transcriptome profiling approaches (Archer® FusionPlex® Sarcoma Kit), which led to the identification of an infantile glioma case harboring a novel *ROS1* fusion.

Design: We searched our database of 238 patients with glioma, enrolled in an IRB-approved study for Precision Medicine. Pathological diagnoses, results of RNA-seq and whole exome sequencing were reviewed. To support identification of novel fusions or gene partners, we further interrogated a subset of cases by targeted transcriptome sequencing. An additional 513 adult lower grade infiltrating gliomas and 592 glioblastomas from the TCGA dataset were screened to examine the frequency of the identified fusion events.

Results: RNA-seq nominated 5 novel fusions involving oncogenes (Table 1), including a *GLI1* fusion in case 1; however, the un-targeted and targeted methods disagreed on the fusion partner. Both methods identified a *PHIP-ROS1* fusion in a pediatric high-grade astrocytoma (case 2, Figure 1). The *PHIP-ROS1* fusion was predicted to be in-frame with preservation of the entire ROS1 kinase domain, suggesting that it may could be susceptible to tyrosine kinase inhibitors (Figure 2). We had noted an 8p gain in this case using WES; however, no major oncogenic mutations were identified prior to RNA sequencing. Only one *ROS1* fusion, *CEP85L-ROS1*, was observed in an adult glioblastoma case in TCGA dataset.

Table 1. **Gene Fusions by Case.** Gliomas with both un-targeted and targeted RNA-seq (custom Archer® FusionPlex® Sarcoma Kit).

Case	Age	Sex	Diagnosis	Un-targeted RNA-seq (Whole transcriptome)			Targeted RNA-seq (Archer)		
				left gene	right gene	Fusion effect	left gene	right gene	Fusion effect
1	59 y.o.	M	Glioblastoma	*MDM4*	*GLI1*	5UTR-5UTR	*GLI1*	*ATP2B2; KAZN*	in-frame
2	5 m	F	pediatric high-grade astrocytoma	*PHIP*	*ROS1*	in-frame	*PHIP*	*ROS1*	in-frame
3	78 y.o.	M	Glioblastoma	*GPSM2*	*NTRK2*	out-of-frame	*None detected*		
4	71 y.o.	M	Glioblastoma	*ATP10D*	*TEK*	out-of-frame	*None detected*		
5	62 y.o.	M	Glioblastoma	*NTRK2*	*CLU*	5UTR-exon	*None detected*		

Figure 1 - 858

Figure 1. Novel PHIP-ROS1 fusion in a pediatric infiltrating glioma.
Histopathology of pediatric high-grade astrocytoma is shown (frozen section H&E slide; 10x and 20x original magnification).

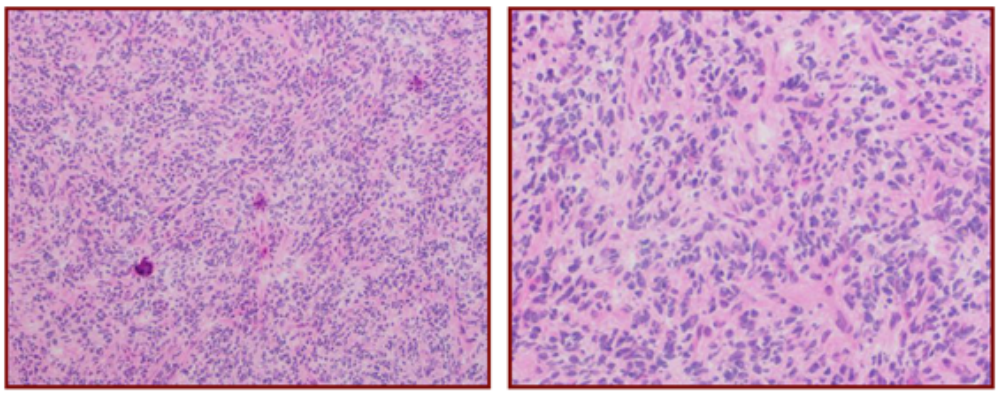

Figure 2 - 858

Figure 2. The schematic diagram of the novel PHIP-ROS1 in-frame fusion is illustrated.

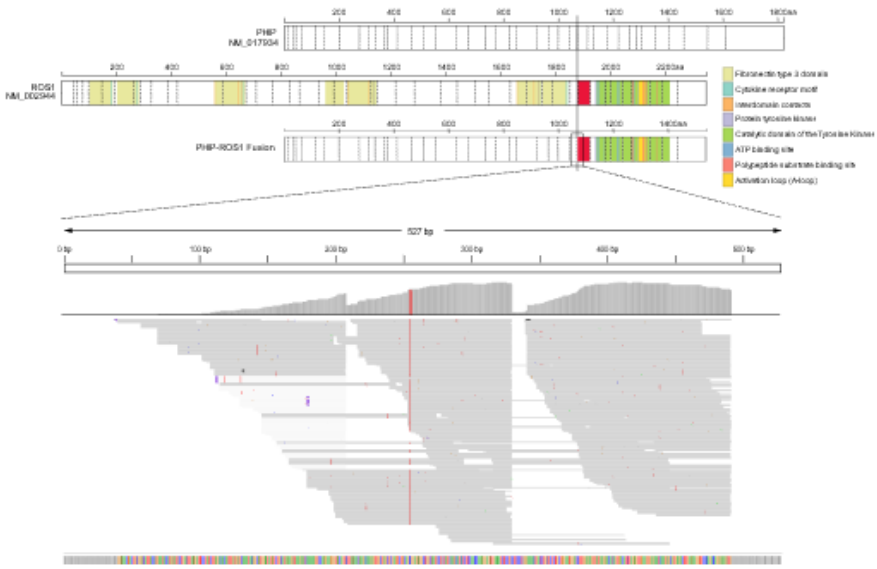

Conclusions: In this study, we identified a novel *ROS1* fusion with a structure that suggests that it could be susceptible to inhibition with tyrosine kinase inhibitors. While *ROS1* fusions have been previously described in pediatric and adult gliomas, *PHIP* is a novel *ROS1* fusion partner. A potential novel fusion involving *GLI1* was also identified. Orthogonal validation is ongoing. Identification of novel potentially targetable fusions will be more frequent as highly sensitive transcriptome methods are applied.

859 Does Well Differentiated Neuroendocrine Tumor(NET) G1 Exist In The Pituitary Glands?

Robert Osamura[1], Chie Inomoto[2], Midori Matsuda[3], Shigeyuki Tahara[4], Kenichi Oyama[3], Akira Matsuno[5], Akira Teramoto[4]

[1]Nippon Koukan Hospital, Kawasaki, Japan, [2]Tokai University, Tokyo, Japan, [3]Teikyo University School of Medicine, Itabashi, Japan, [4]Nippon Medical School, Tokyo, Japan, [5]Teikyo University School of Medicine, Tokyo, Japan

Disclosures: Robert Osamura: None; Chie Inomoto: None; Midori Matsuda: None; Shigeyuki Tahara: None; Kenichi Oyama: None; Akira Matsuno: None; Akira Teramoto: None

Background: After the 4th WHO endocrine tumor classification was published in 2017, the concept of common nomenclature, NET & NEC, for the neuroendocrine neoplasms (NENs) of various organs was introduced (Mod Pathol 2018, Endocr Relat Cancer 2020). Since then, it has been suggested that the pituitary adenomas could be designated as PitNET in NENs. This study is aimed at to clarify whether the morphological NET G1 does exist in the pituitary which is equivalent to the pancreas and gut(WHO 2017, 2019).

Design: According to WHO 2017 and 2019, NET G1 is defined as well differentiated neuroendocrine morphology(rosette,pseudorosette,ribbon-like,cords and organoid) and low(<3%) Ki-67 indices. Our study is aimed at to detect NET G1 in the pituitary adenomas and to analyze the clinical and pathological characteristics.

Our large series of the pituitary adenomas were reviewed to detect the cases equivalent to pancreatic or gut NET G1(see above). The selected cases were subjected to immunohistochemical staining for pituitary hormones, Ki-67, Insulinoma-associated protein 1(INSM1; neuroendocrine marker), Somatostatin receptor(SSTR)2,5 and transcription factors(SF1, Pit1). Clinical information such as Knosp grading was also evaluated.

Results: Total nine cases satisfied the criteria of NET G1. Case 6 demonstrated representative morphology(Fig. 1 H&E stain) and the tumor cells were immunohistochemically positive for INSM1, FSH, αSU and Ki-67 index was 2%(Fig, 2). Clinical and pathological features of these nine cases are summarized in Table 1. All cases were male and 8 cases were either Knosp grading 1 or 2. One case was grade 3. INSM1 was positive in all cases with various intensity. Eight cases were immunohistochemically positive for FSH and seven cases for αSU. All cases were positive for SSTR2 but only one case was positive for SSTR5. SF1 was positive in 5 of 6 cases. Pit1 was positive in cases 1 and 9. In Case 9, the tumor cells were positive for GH, PRL,TSH and αSU as well as Pit1 and SF1. These features were suggestive of plurihormonal Pit1 positive adenoma(WHO 2017).

Table 1 Nine cases of NETG1 in the pituitary

Cases	M/F	Age	Knosp	GH	PRL	ACTH	FSH	LH	TSH	aSU	Ki-67	SSTR2	SSTR5	INSM1
1	M	66	2	-	-	-	4+	-	-	-	1	2+	-	+++
2	M	58	2	-	-	-	2+	-	-	2+	2.2	2+	-	+++
3	M	43	2	-	-	-	+	+	-	2+	2.3	2+	-	+++
4	M	75	3	-	-	-	++	-	-	-	<1	3+	-	+++
5	M	64	2	-	-	-	1+	-	-	2+	2	2+	-	+++
6	M	31	1	-	-	-	4+	-	-	1+	2	2+	-	+
7	M	44	2	-	-	-	4+	-	-	+	2	2+	-	++
8	M	70	3	-	-	-	3+	2+	-	+	<1	3+	-	+
9	M	44	1	+	2+	-	+	-	+	3+	1	3+	2+	+

Immunohistochemistry:-:negative 1+ weak positive 2+:intermediate low 3+:Intermediate high 4+:intense
INSMI immunohistochemistry:+:weak ++:intermediate +++:intense
Ki-67 index %

Figure 1 - 859

Fig. 1 Case 6 Histology of NET G1 of the pituitary(H&E stain)

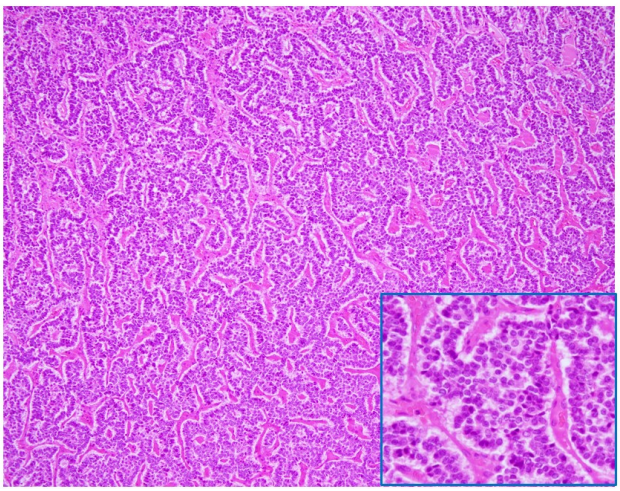

Figure 2 - 859

Fig. 2 Case 6 Immunohistochemistry of NET G1 in the pituitary

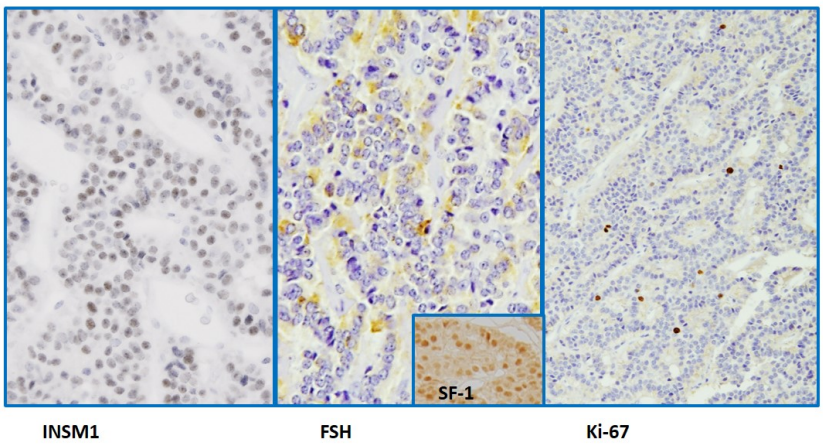

Conclusions: Our study clearly showed the existence of NET G1 in the pituitary glands as it has been suggested.(2020). The majority of the cases were in the gonadotroph lineage, but expression of SSTR and Pit1 may suggest some heterogeneity. We need further clinical and pathological evidence before we incorporate the terminology of PitNET G1 as an entity. It should be also emphasized that PitNET G1 should not be confused with the metastatic NET G1 from pancreas or gut.

860 Epithelioid Glioblastoma and Pleomorphic Xanthoastrocytoma: Molecular Classification of Two Morphologically Similar Glial Neoplasms

Sharika Rajan[1], Zied Abdullaev[2], Martha Quezado[2], Kenneth Aldape[2]
[1]National Cancer Institute, National Institutes of Health, Bethesda, MD, [2]National Institutes of Health, Bethesda, MD

Disclosures: Sharika Rajan: None; Martha Quezado: None

Background: Histomorphological differentiation between glioblastoma (GBM), epithelioid subtype and pleomorphic xanthoastrocytoma (PXA) is often challenging. Currently it appears that molecular evaluation can aid in this differentiation and in particular methylation profiling. In this study, we systematically evaluate a cohort of neoplasms

categorized as epithelioid GBM and PXA, closely analyzing their methylation profiling subclassification in an attempt to identify a molecular signature that could separate these entities.

Design: 38 cases received at our institution for molecular studies and diagnosed on H&E as epithelioid GBM, (anaplastic) PXA, and glioneuronal tumors not further classified were studied. Each case was screened for: presence of epithelioid/rhabdoid-like cells and xanthomatous cells, nuclear pleomorphism, intranuclear inclusions, eosinophilic granular bodies (EGB), increased perivascular lymphocytes, and reticulin fibers. Features of high-grade glial neoplasm: glomeruloid vascular proliferation, increased mitoses and pseudopalisading necrosis were also noted. DNA from tumor was extracted and analyzed using the Illumina MethylationEPIC BeadChip (850k) array. Copy number profiles were generated using the "conumee" package for R. *MGMT* promoter methylation status and mutation analysis for the *TERT* promoter regions were evaluated.

Results: 38 cases (23 females, 15 males), mean age 31 ± 18 was analyzed. On histopathology, nuclear pleomorphism was noted in most cases (33/38, 87%), intranuclear inclusions in (14/38, 37%), lymphoplasmacytic infiltrates in 13/38 (34%), EGB in 9/38 (24%), xanthomatous changes in 5/38 (13%), and necrosis in 18/38 (47%), out of which pseudopalisading was seen in 10 cases. DNA methylation classifier on these 38 cases indicated that 17 tumors (45%) classified as PXA/anaplastic PXA with a high confidence score (>0.8). Remaining 21 cases classified as PXA with lower confidence score and/or the t-SNE plots of these cases placed the tumor in the general area of PXA. Mutation screening revealed, 26/36 assessed cases had a BRAF V600E mutation; 3 cases had *TERT* promoter mutation and 3 had *MGMT* promoter methylation present. 28 cases had homozygous loss of gene CDKN2A/2B, and while isolated gain of ch7 or loss of ch 10 were noted on copy number analysis, the combination of *TERT* promoter mutation with +7/-10 was not identified.

Conclusions: DNA methylation classifier profiling revealed a set of cases were classifiable as (anaplastic) PXA with very high to lower confidence score. Some of these tumors lack classic PXA features, some of which with pseudopalisading necrosis, yet they show the molecular profile of PXA, and do not show a profile of GBM. Most of these tumors harbor a BRAF V600E mutation and homozygous loss of gene CDKN2A/2B. We recommend that tumors with overlapping epithelioid GBM and PXA morphology should be further investigated with methylation and molecular profiling.

861 Cervicomedullary Astroblastoma with EWSR1-BEND2 Fusion: Expanding the Molecular Heterogeneity of Astroblastomas and the HGNET-MN1 Methylation Class Family

Jose Velazquez Vega[1], Anna Janss[1], William Boydston[1], Julia Bridge[2], Matija Snuderl[3], Matthew Schniederjan[4]
[1]Children's Healthcare of Atlanta, Atlanta, GA, [2]University of Nebraska Medical Center, Omaha, NE, [3]New York University, New York, NY, [4]Emory University, Children's Healthcare of Atlanta, Atlanta, GA

Disclosures: Jose Velazquez Vega: None; William Boydston: None; Julia Bridge: None

Background: In 2016, four new central nervous system (CNS) tumor entities were described following DNA methylation analysis of CNS primitive neuroepithelial tumors. One of these entities was termed CNS high-grade neuroepithelial tumor with MN1 alteration (CNS HGNET-MN1). Astroblastomas arising in the pediatric population are enriched for MN1 alterations and often classify with the CNS HGNET-MN1 on DNA methylation analysis. *MN1-BEND2* and *MN1-CXXC5* gene fusions were identified in these tumors. Despite some unresolved issues with the terminology of CNS HGNET-MN1 tumors, CIMPACT-NOW has recommended the inclusion of 'Astroblastoma, MN1-altered' in future WHO classifications.

Design: A 17-yeal-old female presented with 6 months of worsening dysphagia, respiratory difficulty and changes in ambulation. Neurologic exam revealed brainstem deficits and brain MRI showed an intra-axial solid and cystic mass at the cervicomedullary junction. Only the solid component was contrast enhancing. The patient underwent subtotal resection and had stable disease for 3.5 years before asymptomatic gradual progression. Partial re-resection was performed at nearly four years after the first surgery. There has been no systemic chemotherapy. Proton bean radiotherapy was started after the second surgery. The patient is alive with stable disease at 4.5 years since first diagnosed.

Results: Both specimens showed similar histology albeit with comparatively increased cellularity and proliferation in the re-excision material. Sections reveal a markedly sclerotic neoplasm with variably epithelioid tumor cells with eosinophilic to clear cytoplasm and with perivascular affinity imparting a pseudopapillary growth pattern. Prominent vascular hyalinization with ribbon-like arrangements and astroblastic pseudorosettes were noted. Nuclear pleomorphism and intranuclear inclusions were seen in the first specimen. There was no necrosis or microvascular proliferation. Up to 2 mitoses per 10HPF were seen in the second specimen. By immunohistochemistry the tumor was positive for GFAP, S100 (focal), EMA (membranous), CD99 (membranous), TLE1, SATB2, BCOR, CyclinD1, AE1/AE3 (focal), SOX10 (focal), and synaptophysin (rare cells). INI1 and BRG1 nuclear expression was retained. Immunohistochemistry was negative for CAM5.2 and BRAF VE1. The Ki-67 proliferation index was initially estimated at 2-3% and was about 10% in the second resection material. Molecular inversion probe array showed whole chromosomal losses of 1, 10, 13, 14, 18, 21, and 22 and partial loss of chromosome X.
An *EWSR1/BEND2* fusion was identified by next generation sequencing. The tumor classified as HGNET-MN1 methylation class with a calibrated score of 0.98.

Conclusions: Our case represents the second case of cervicomedullary astroblastoma with an *EWSR1/BEND2* fusion which also classified as HGNET-MN1 methylation class despite the absence of an MN1 alteration (PMID: 31863478).

862 Utility of ISL1 in Pituitary Tumors

Martin Wartenberg[1], Theoni Maragkou[1], Sabina Berezowska[2], Ekkehard Hewer[3]
[1]Institut of Pathology, University of Bern, Bern, Switzerland, [2]Institute of Pathology, CHUV, Lausanne, Switzerland, [3]CHUV and University of Lausanne, Lausanne, Switzerland

Disclosures: Martin Wartenberg: None; Theoni Maragkou: None; Sabina Berezowska: None; Ekkehard Hewer: None

Background: The clinical and biological heterogeneity of pituitary neuroendocrine tumors (PitNET) mirrors distinct histogenetic lineages characterized by specific transcription factor expression profiles. In the context of diagnostic immunohistochemistry, these transcription factors are increasingly supplementing pituitary hormones for accurate classification of PitNETs. Furthermore, these markers are of diagnostic utility in distinguishing PitNETs from mimics, especially in the context of locally extensive or metastatic disease. ISL1 is a transcription factor involved in pituitary development, but its expression in adult pituitary or PitNET has not been systematically studied. The observation of expression of ISL1, which in a diagnostic context is notably used as a marker of pancreatic neuroendocrine tumors, prompted us to further investigate its expression pattern across PitNET subtypes as well as in non-neoplastic pituitary.

Design: PitNETs were assessed by tissue microarray technique for expression of ISL1 by immunohistochemistry. Additional samples representing less common PitNET subtypes were analyzed through immunohistochemistry of full slides. Subsequently, we included ISL1 in our routine pituitary immunohistochemistry panel in order to validate its performance in a clinical setting in a series of 49 consecutive cases and to assess its expression patterns relative to pituitary transcription factors Pit-1 and SF-1.

Results: Nearly all PitNETs showed either diffuse ISL1 positivity or lacked ISL1 immunoreactivity entirely. ISL1 expression was frequently present in gonadotroph tumors (41/44; 93 %) and also observed in thyrotroph tumors (3/3). Staining intensity was usually strong, notably also in gonadotroph tumors with only weak and/or focal expression of SF-1. Conversely, ISL1 expression was uncommon in Pit-1 lineage (somatotroph, lactotroph, plurihormonal) tumors (2/25; 8%) and corticotroph tumors (1/6; 17%). Non-neoplastic anterior pituitary tissue present in surgical specimens displayed a heterogeneous staining pattern, consistent with that of LH/FSH-producing cells.

Conclusions: ISL1 is frequently expressed in both gonadotrophic PitNET as well as TSH-positive tumors (uni- or plurihormonal). Since expression is usually strong and diffuse, it may contribute favorably to a diagnostic panel for classification of PitNET. Awareness of this immunophenotype may help to correctly identify a pituitary origin in case of locally extensive or metastatic disease.